EUROPEAN ORGANIZATION FOR NUCLEAR RESEARCH

CERN-PPE/93-09
January 15, 1993

Measurement of the τ lifetime

The OPAL Collaboration

Abstract

The τ lifetime has been measured with the OPAL detector at LEP, from analyses using the impact parameters in decays to single charged tracks, and the decay lengths from τ decays to three charged tracks. The 1991 sample of approximately 12300 τ-pair events, of which 70% contain silicon microvertex detector information, has been combined with a re-analysis of the 5100 events recorded during 1990. The two statistically-independent determinations give:

$$\tau(\text{one-prong}) = 296.4 \pm 7.1(\text{stat}) \pm 3.8(\text{sys}) \text{ fs},$$

$$\tau(\text{three-prong}) = 286.3 \pm 7.4(\text{stat}) \pm 5.2(\text{sys}) \text{ fs}.$$

The weighted average of these results after combination of the uncorrelated systematic errors is:

$$\tau_\tau = 291.9 \pm 5.1(\text{stat}) \pm 3.1(\text{sys}) \text{ fs}.$$

(To be submitted to Physics Letters B)

The OPAL Collaboration

P.D. Acton[25], G. Alexander[23], J. Allison[16], P.P. Allport[5], K.J. Anderson[9], S. Arcelli[2], A. Astbury[28], D. Axen[29], G. Azuelos[18,a], G.A. Bahan[16], J.T.M. Baines[16], A.H. Ball[17], J. Banks[16], R.J. Barlow[16], S. Barnett[16], J.R. Batley[5], G. Beaudoin[18], A. Beck[23], G.A. Beck[13], J. Becker[10], T. Behnke[27], K.W. Bell[20], G. Bella[23], P. Bentkowski[18], P. Berlich[10], S. Bethke[11], O. Biebel[3], U. Binder[10], I.J. Bloodworth[1], P. Bock[11], B. Boden[3], H.M. Bosch[11], H. Breuker[8], P. Bright-Thomas[25], R.M. Brown[20], A. Buijs[8], H.J. Burckhart[8], C. Burgard[27], P. Capiluppi[2], R.K. Carnegie[6], A.A. Carter[13], J.R. Carter[5], C.Y. Chang[17], D.G. Charlton[8], S.L. Chu[4], P.E.L. Clarke[25], I. Cohen[23], J.C. Clayton[1], W.J. Collins[5], J.E. Conboy[15], M. Cooper[22], M. Coupland[14], M. Cuffiani[2], S. Dado[22], G.M. Dallavalle[2], S. De Jong[13], L.A. del Pozo[5], H. Deng[17], A. Dieckmann[11], M. Dittmar[4], M.S. Dixit[7], E. do Couto e Silva[12], J.E. Duboscq[8], E. Duchovni[26], G. Duckeck[11], I.P. Duerdoth[16], D.J.P. Dumas[6], P.A. Elcombe[5], P.G. Estabrooks[6], E. Etzion[23], H.G. Evans[9], F. Fabbri[2], M. Fierro[2], M. Fincke-Keeler[28], H.M. Fischer[3], D.G. Fong[17], M. Foucher[17], A. Gaidot[21], O. Ganel[26], J.W. Gary[4], J. Gascon[18], R.F. McGowan[16], N.I. Geddes[20], C. Geich-Gimbel[3], S.W. Gensler[9], F.X. Gentit[21], G. Giacomelli[2], R. Giacomelli[2], V. Gibson[5], W.R. Gibson[13], J.D. Gillies[20], J. Goldberg[22], M.J. Goodrick[5], W. Gorn[4], C. Grandi[2], F.C. Grant[5], J. Hagemann[27], G.G. Hanson[12], M. Hansroul[8], C.K. Hargrove[7], P.F. Harrison[13], J. Hart[8], P.M. Hattersley[1], M. Hauschild[8], C.M. Hawkes[8], E. Heflin[4], R.J. Hemingway[6], R.D. Heuer[8], J.C. Hill[5], S.J. Hillier[8], T. Hilse[10], D.A. Hinshaw[18], J.D. Hobbs[8], P.R. Hobson[25], D. Hochman[26], R.J. Homer[1], A.K. Honma[28,a], R.E. Hughes-Jones[16], R. Humbert[10], P. Igo-Kemenes[11], H. Ihssen[11], D.C. Imrie[25], A.C. Janissen[6], A. Jawahery[17], P.W. Jeffreys[20], H. Jeremie[18], M. Jimack[2], M. Jobes[1], R.W.L. Jones[13], P. Jovanovic[1], C. Jui[4], D. Karlen[6], K. Kawagoe[24], T. Kawamoto[24], R.K. Keeler[28], R.G. Kellogg[17], B.W. Kennedy[15], S. Kluth[5], T. Kobayashi[24], D.S. Koetke[8], T.P. Kokott[3], S. Komamiya[24], L. Köpke[8], J.F. Kral[8], R. Kowalewski[6], J. von Krogh[11], J. Kroll[9], M. Kuwano[24], P. Kyberd[13], G.D. Lafferty[16], R. Lahmann[17], F. Lamarche[18], J.G. Layter[4], P. Leblanc[18], A.M. Lee[17], M.H. Lehto[15], D. Lellouch[26], C. Leroy[18], J. Letts[4], S. Levegrün[3], L. Levinson[26], S.L. Lloyd[13], F.K. Loebinger[16], J.M. Lorah[17], B. Lorazo[18], M.J. Losty[7], X.C. Lou[12], J. Ludwig[10], M. Mannelli[8], S. Marcellini[2], G. Maringer[3], C. Markus[3], A.J. Martin[13], J.P. Martin[18], T. Mashimo[24], P. Mättig[3], U. Maur[3], J. McKenna[28], T.J. McMahon[1], J.R. McNutt[25], F. Meijers[8], D. Menszner[11], F.S. Merritt[9], H. Mes[7], A. Michelini[8], R.P. Middleton[20], G. Mikenberg[26], J. Mildenberger[6], D.J. Miller[15], R. Mir[12], W. Mohr[10], C. Moisan[18], A. Montanari[2], T. Mori[24], M. Morii[24], T. Mouthuy[12,b], B. Nellen[3], H.H. Nguyen[9], M. Nozaki[24], S.W. O'Neale[1], F.G. Oakham[7], F. Odorici[2], H.O. Ogren[12], C.J. Oram[28,a], M.J. Oreglia[9], S. Orito[24], J.P. Pansart[21], B. Panzer-Steindel[8], P. Paschievici[26], G.N. Patrick[20], N. Paz-Jaoshvili[23], P. Pfister[10], J.E. Pilcher[9], J. Pinfold[31], D. Pitman[28], D.E. Plane[8], P. Poffenberger[28], B. Poli[2], A. Pouladdej[6], T.W. Pritchard[13], H. Przysiezniak[18], G. Quast[27], M.W. Redmond[9], D.L. Rees[8], G.E. Richards[16], D. Robinson[8], A. Rollnik[3], J.M. Roney[28,c], E. Ros[8], S. Rossberg[10], A.M. Rossi[2], M. Rosvick[28], P. Routenburg[6], K. Runge[10], O. Runolfsson[8], D.R. Rust[12], M. Sasaki[24], C. Sbarra[8], A.D. Schaile[10], O. Schaile[10], W. Schappert[6], P. Scharff-Hansen[8], P. Schenk[4], B. Schmitt[3], H. von der Schmitt[11], S. Schreiber[3], C. Schwick[27], J. Schwiening[3], W.G. Scott[20], M. Settles[12], T.G. Shears[5], B.C. Shen[4], C.H. Shepherd-Themistocleous[7], P. Sherwood[15], R. Shypit[29], A. Simon[3], P. Singh[13], G.P. Siroli[2], A. Skuja[17], A.M. Smith[8], T.J. Smith[28], G.A. Snow[17], R. Sobie[28,c], R.W. Springer[17], M. Sproston[20], K. Stephens[16], J. Steuerer[28], R. Ströhmer[11], D. Strom[30], T. Takeshita[24,d], P. Taras[18], S. Tarem[26], M. Tecchio[9], P. Teixeira-Dias[11], N. Tesch[3], N.J. Thackray[1], M.A. Thomson[15], E. Torrente-Lujan[22], G. Transtromer[25], N.J. Tresilian[16], T. Tsukamoto[24], M.F. Turner[8], G. Tysarczyk-Niemeyer[11], D. Van den plas[18], R. Van Kooten[27], G.J. VanDalen[4], G. Vasseur[21], C.J. Virtue[7], A. Wagner[27], D.L. Wagner[9], C. Wahl[10], J.P. Walker[1], C.P. Ward[5], D.R. Ward[5], P.M. Watkins[1], A.T. Watson[1], N.K. Watson[8], M. Weber[11], P. Weber[6], P.S. Wells[8], N. Wermes[3], M.A. Whalley[1], G.W. Wilson[4], J.A. Wilson[1], V-H. Winterer[10], T. Wlodek[26], S. Wotton[11], T.R. Wyatt[16], R. Yaari[26], A. Yeaman[13], G. Yekutieli[26], M. Yurko[18], W. Zeuner[8], G.T. Zorn[17].

[1]School of Physics and Space Research, University of Birmingham, Birmingham, B15 2TT, UK
[2]Dipartimento di Fisica dell' Università di Bologna and INFN, Bologna, 40126, Italy
[3]Physikalisches Institut, Universität Bonn, D-5300 Bonn 1, FRG
[4]Department of Physics, University of California, Riverside, CA 92521 USA
[5]Cavendish Laboratory, Cambridge, CB3 0HE, UK
[6]Carleton University, Dept of Physics, Colonel By Drive, Ottawa, Ontario K1S 5B6, Canada
[7]Centre for Research in Particle Physics, Carleton University, Ottawa, Ontario K1S 5B6, Canada
[8]CERN, European Organisation for Particle Physics, 1211 Geneva 23, Switzerland
[9]Enrico Fermi Institute and Department of Physics, University of Chicago, Chicago Illinois 60637, USA
[10]Fakultät für Physik, Albert Ludwigs Universität, D-7800 Freiburg, FRG
[11]Physikalisches Institut, Universität Heidelberg, Heidelberg, FRG
[12]Indiana University, Dept of Physics, Swain Hall West 117, Bloomington, Indiana 47405, USA
[13]Queen Mary and Westfield College, University of London, London, E1 4NS, UK
[14]Birkbeck College, London, WC1E 7HV, UK
[15]University College London, London, WC1E 6BT, UK
[16]Department of Physics, Schuster Laboratory, The University, Manchester, M13 9PL, UK
[17]Department of Physics, University of Maryland, College Park, Maryland 20742, USA
[18]Laboratoire de Physique Nucléaire, Université de Montréal, Montréal, Quebec, H3C 3J7, Canada
[20]Rutherford Appleton Laboratory, Chilton, Didcot, Oxfordshire, OX11 0QX, UK
[21]DAPNIA/SPP, Saclay, F-91191 Gif-sur-Yvette, France
[22]Department of Physics, Technion-Israel Institute of Technology, Haifa 32000, Israel
[23]Department of Physics and Astronomy, Tel Aviv University, Tel Aviv 69978, Israel
[24]International Centre for Elementary Particle Physics and Dept of Physics, University of Tokyo, Tokyo 113, and Kobe University, Kobe 657, Japan
[25]Brunel University, Uxbridge, Middlesex, UB8 3PH UK
[26]Nuclear Physics Department, Weizmann Institute of Science, Rehovot, 76100, Israel
[27]Universität Hamburg/DESY, II Inst für Experimental Physik, 2000 Hamburg 52, Germany
[28]University of Victoria, Dept of Physics, P O Box 3055, Victoria BC V8W 3P6, Canada
[29]University of British Columbia, Dept of Physics, 6224 Agriculture Road, Vancouver BC V6T 1Z1, Canada
[30]University of Oregon, Dept of Physics, Eugene, Oregon 97403, USA
[31]University of Alberta, Dept of Physics, Edmonton AB T6G 2J1, Canada

[a]Also at TRIUMF, Vancouver, Canada V6T 2A3
[b]Now at Centre de Physique des Particules de Marseille, Faculté des Sciences de Luminy, Marseille
[c]And IPP, University of Victoria, Dept of Physics, P O Box 3055, Victoria BC V8W 3P6, Canada
[d]Also at Shinshu University, Matsumoto 390, Japan

1 Introduction

In the Standard Model of electroweak interactions there exist well-defined relations between the lifetime of the τ lepton, its mass, and its electronic and muonic branching ratios [1]. For example, the τ lifetime, τ_τ, can be predicted from the muon mass and lifetime, m_μ and τ_μ, and the τ mass, m_τ, using

$$\tau_\tau = \tau_\mu \left(\frac{g_\mu}{g_\tau}\right)^2 \left(\frac{m_\mu}{m_\tau}\right)^5 \mathrm{BR}(\tau \to \nu_\tau \overline{\nu}_e \mathrm{e}). \quad (1)$$

Here g_μ and g_τ are the electroweak charged current couplings of the μ and τ leptons, which are equal under the assumption of lepton universality. In this case, current experimental determinations of the remaining parameters in equation (1) lead to a discrepancy of more than two standard deviations between the measured and predicted τ lifetimes — the so-called "τ decay puzzle" [2]. Furthermore, this anomaly remains at the same level even with the inclusion of the new and very precise measurements of the τ lepton mass [3, 4]. Were such a discrepancy to remain even after improved experimental determinations of the τ lifetime it could be the signal for new physics, such as a very massive fourth generation neutrino or the breakdown of lepton universality.

We present a new measurement of the τ lifetime from a direct combination of two statistically independent techniques applied to the combined 1990 and 1991 OPAL data samples, which supercedes the previously published OPAL result for the 1990 data [5]. The first method is based on the impact parameter distribution of one-prong τ decay tracks, while the second measures the decay length of three-prong τ decay vertices. In addition we include the result of a novel lifetime measurement technique based on the 1-3 τ decay topology, which is independent of beam spot information. A brief description of the OPAL detector is followed by discussions of the event selection, τ-pair Monte Carlo, and determination of the beam position and size. The one-prong, three-prong, and 1-3 lifetime measurements are then described. We conclude with the combined result and a discussion of its implications for the τ decay puzzle.

2 The OPAL detector

OPAL is an $\mathrm{e^+e^-}$ experiment collecting data at center-of-mass energies near the $\mathrm{Z^0}$ peak, $\sqrt{s} \simeq 91.16$ GeV. Approximately 78% of the data used in these analyses were collected at the nominal peak energy, with the remainder being collected during energy scans within a few GeV of the peak energy. A complete description of the OPAL detector is found in references [6, 7]. We describe briefly the aspects of the detector pertinent to this analysis. The coordinate system is defined so that the z-axis follows the electron beam direction and the x-y plane is perpendicular to it with the x-axis lying horizontally in the plane of the LEP ring. The polar angle θ is defined relative to the $+z$-axis, while the azimuthal angle ϕ is defined relative to the $+x$-axis. The radius, r, is the distance from the z-axis.

The portion of the central tracking system common to all data sets comprises a precision vertex chamber, jet chamber and z-chambers. The cylindrical vertex drift chamber consists of 36 azimuthal sectors each having 12 axial wires, at equally-spaced radial intervals from 10.3 cm

to 16.2 cm, and 6 stereo wires, at radii from 18.8 cm to 21.3 cm. The stereo wires are canted by 4° to provide z information. The detector has multiple hit capability, with spatial resolutions of 50 μm and 90 μm for the first and subsequent hits on the anode wires, respectively. The large-volume jet drift chamber contains 159 layers of axial anode wires, each providing hit resolutions of about 130 μm in the r-ϕ plane. The z-chambers provide accurate z-coordinate measurements in the barrel region of the detector, $|\cos\theta| < 0.72$. The central tracking chambers are contained in a 4 bar pressure vessel immersed in a solenoidal magnetic field of 0.435 T. The impact parameter resolution achieved for 45 GeV/c μ-pair and Bhabha events is 40 μm using the drift chambers alone. Time-of-flight counters and a lead-glass electromagnetic calorimeter are located beyond the coil. The electromagnetic calorimeter system provides coverage over nearly the full solid angle, for $|\cos\theta| \leq 0.98$. Hadron calorimeter and muon detection systems are located beyond the electromagnetic calorimeter.

A 1.4 mm-thick carbon fiber beam pipe of 7.8 cm radius was in place for the 1990 LEP run. For the 1991 run a high precision silicon microvertex detector [7] surrounding a 5.3 cm-radius beryllium-composite beam pipe was inserted into the carbon fiber pipe. The silicon detector was operational for 73% of the data collected in 1991. The detector provides two layers of silicon strip readout in the r-ϕ plane. The two layers are formed by concentric polygons of detector "ladders" at radii of 6.1 and 7.5 cm. The inner layer has 11 ladders, and the outer has 14. Each ladder comprises 629 channels at a readout pitch of 50 μm, in an active width of slightly more than 3 cm and active length of 18 cm. This corresponds to an acceptance of $|\cos\theta| \leq 0.8$. Within this acceptance, the probability for tracks in τ-pair events to contain at least one silicon hit, including dead channel inefficiencies, is 90%. The intrinsic detector resolution is about 5 μm [7]. However, alignment uncertainties within OPAL currently limit the space-point resolution to about 12 μm. When combined with the angle and curvature information provided by the central drift chambers this results in an impact parameter resolution of 18 μm in μ-pair and Bhabha events.

3 The τ-pair data selection and Monte Carlo simulation

The OPAL detector recorded 7 pb^{-1} integrated luminosity during 1990, and 14 pb^{-1} during 1991. Tau-pair events were selected by requiring two collimated, back-to-back low multiplicity jets. Full details of the selection are given elsewhere [8], and we give here only a general overview of the cuts. Events were required to have the event thrust axis lying within the detector acceptance, $|\cos\theta_{\rm thrust}| < 0.9$, with a visible energy less than 80% of the center-of-mass energy. The maximum allowed number of charged tracks was 7, and the maximum number of charged tracks and electromagnetic clusters combined was 16. The multiplicity cuts aid in rejecting multihadronic events. The event total energy was used to reject Bhabha and two-photon backgrounds, and cosmic rays were rejected with time-of-flight information. Events with visible energy greater than 60% of the center-of-mass energy which contained two tracks identified as muons were rejected as μ-pair candidates.

The initial selection found 17553 candidates in the full data sample. The lifetime analyses require good beam position information according to the algorithm described in the following section, which resulted in the rejection of 149 of these events. The remaining sample contained

17404 τ-pair candidates, of which 5107 came from the 1990 data and 12297 came from the 1991 data.

Data used in the lifetime analyses were subjected to further cuts intended to reduce the relevant backgrounds for each sample. For the one-prong analysis the acoplanarity angle between the summed momentum vectors of the event hemispheres, as defined by the plane perpendicular to the thrust axis, was required to exceed 2 mrad, in order to reduce the contributions from μ-pair, Bhabha, and two-photon events. The tracks from one-prong decays were then required to have: 1) at least 6 axial-layer vertex chamber hits, or at least one silicon detector hit, 2) at least half the geometrically possible number of hits in the central jet chamber, and 3) track impact parameter error, including the beam size contribution, of less than 0.1 cm. The 0.6% of events in which the two τ candidates appeared to decay into single tracks of the same measured charge were rejected. A total of 25579 tracks remained after all the selection cuts, of which 7537 (29.5%) came from the 1990 data, 7148 (27.9%) came from the 1991 data without silicon hits on the tracks, and 10894 (42.6%) came from the 1991 data having at least one silicon hit in the track fit.

For the three-prong analysis, multihadron background suppression was provided by a veto on events which are tagged by the standard OPAL $Z^0 \to q\overline{q}$ event selection described in reference [8]. According to Monte Carlo studies, these cuts reduce the residual multihadron contamination by 66%, with a loss of only 2.1% of the τ signal. A total of 4677 candidate three-prong τ decays remained after this selection. Tracks originating from photon conversions were eliminated with an invariant mass cut of $M(e^+e^-) < 0.05$ GeV/c^2 for two oppositely-charged tracks with assumed electron masses. This criterion eliminated 567 of the vertex candidates. Tracks from $K^0 \to \pi^+\pi^-$ decays were likewise eliminated by a mass cut, 0.473 GeV/c^2 $< M(\pi^+\pi^-) <$ 0.523 GeV/c^2, which removed 82 additional vertex candidates. The total number of three-prong decay candidates remaining for the lifetime measurement was 4028, where 1138 (28.3%) came from the 1990 data, 791 (19.6%) came from the 1991 data without the silicon detector, and 2099 (52.1%) came from the 1991 data which have silicon information available.

The background contributions for the one-prong and three-prong decay samples used in the lifetime analyses were estimated with standard Monte Carlo generator programs [9, 10, 11, 12], and are shown in Table 1. The OPAL detector response was simulated with a program [13] that treated in detail the detector material and geometry, as well as the efficiencies and responses of the detector elements. The Monte Carlo tracking resolution was smeared by the additional amounts needed to bring the impact parameter error distributions into agreement for each of the detector configuration.

The KORALZ Monte Carlo program, version 3.8 [12], was used for the simulation of $e^+e^- \to \tau^+\tau^-$ events at $\sqrt{s} = 91.160$ GeV. The program includes multiple QED hard bremsstrahlung and exponentiation of soft photons from the e^+e^- initial state, and single-photon bremsstrahlung from the final state fermions. The only applications of the Monte Carlo for the three-prong analysis involve determination of the slight correction for radiation to the boost factor, $\beta\gamma$, used to convert the measured decay length into the τ lifetime estimation, and evaluation of a small bias described below. For the one-prong analysis, the Monte Carlo determines the calibration curve necessary to extract the lifetime from the measured mean impact parameter. In order to incorporate improvements in determinations of input parameters to

KORALZ certain branching fractions, as well as the mass and width of the a_1 resonance [14] were changed from the program default values. The input τ lifetime and mass were set to the previous world average values of 303.5 fs and 1784 MeV/c^2, respectively [15]. After the same acceptance cuts as were applied to the data, the Monte Carlo samples for the 1990 and 1991 detector configurations contained 37826 and 72113 events, respectively.

4 The beam spot determination

The reconstructed beam spot position was used to estimate the τ production point. It was determined using an iterative procedure described in more detail in reference [5]. All the well-measured tracks from consecutive multihadron and leptonic Z^0 decays were collected until 100 tracks were accumulated. An iterative vertex fit was performed. In these iterations, the track having the largest contribution to the fit χ^2 was discarded until no track contributed more than 10 to the total. After combining consistent beam centroid determinations within individual LEP fills, the precision of determination of the beam coordinates was roughly 15 μm in x and 10 μm in y.

The horizontal beam spread, σ_x, as determined by the above method was 157$\pm$5 μm for the data collected during 1990 and 147$\pm$4 μm for the data collected during 1991. The vertical beam spread, σ_y, was smaller than the typical track impact parameter resolution so the value of 8 μm computed from LEP beam optics was used directly. The extent of the production region was taken as the quadrature sum of the beam spot size and the error on the beam centroid. The uncertainties in the beam position and size are treated in the systematic error evaluations.

The Monte Carlo data for both the 1990 and 1991 samples were generated with beam widths (σ_x, σ_y) =(157,8) μm. The 1991 beam size was rescaled to the value of $\sigma_x = 147$ μm seen in the data. The effects of variations in the Monte Carlo beam widths for the one-prong measurement are discussed in the next section. The three-prong measurement is independent of the Monte Carlo beam size simulation.

5 Lifetime measurement by impact parameter method

The impact parameter, b, of a τ decay track in the x-y plane can be expressed in terms of the flight length, l_{xy}, and the relative azimuthal angle of the track, ψ, with respect to the τ flight direction as $b = l_{xy}|\sin\psi|$. The actual form of the distribution of b resembles an exponential distribution. However, in this analysis, the τ production point is approximated by the beam centroid, and the flight direction by the charged track thrust axis. The b distribution becomes smeared by these effects combined with the detector resolution and acquires negative entries — defined as those in which the track intersects the thrust axis on the opposite side of the beam centroid, rather than in the thrust hemisphere in which it lies. Only the negative impact parameters introduced by the use of the thrust axis direction produce a significant shift in the mean of the b distribution. The tracking resolution and beam size cause a broadening of the measured width of the distribution, without appreciably affecting the mean. Although

the detailed shape of the detected b distribution is difficult to predict, its significant positive shift can be used, by comparison with Monte Carlo prediction, to extract a measurement of the τ lifetime.

In order to avoid the detailed modelling necessary to apply the maximum likelihood method, to remain insensitive to a few mismeasured tracks, and to make efficient use of the available data we have obtained the lifetime from a comparison of the trimmed means of the data and Monte Carlo distributions, i.e. the means of the entries remaining after equal fractions of the highest and lowest impact parameters have been discarded. A 10% total trim factor was chosen. Values of the total trim more than about 30% or less than about 1% lead to an increased statistical error on the trimmed mean, by sheer loss of statistics in the former case and by susceptibility to fluctuations in the sparsely populated tails of the distribution in the latter. The equation for the statistical error on the trimmed mean given in [5, 16] has been corrected.[1] The correct formula for the mean-squared uncertainty on the trimmed mean, $\overline{x}_t$, for total trim t is:

$$s^2_{\overline{x}_t} = \frac{1}{N(1-t)}\left[s^2_t + \frac{t}{4}\left(\frac{(x_{max}-x_{min})^2}{1-t} + (x_{max} - 2\overline{x}_t + x_{min})^2\right)\right] \tag{2}$$

$$s^2_t = \frac{1}{N(1-t)} \sum_{i=N\frac{t}{2}+1}^{N(1-\frac{t}{2})} (x_i - \overline{x}_t)^2, \tag{3}$$

where N is the total number of the individual measurements, x_i, and x_{min}, x_{max} are the minimum, maximum x_i values corresponding to the selected trim value.

The measured value of the 10% trimmed mean, $\overline{x}_{meas}$, gives the lifetime directly from the Monte Carlo trimmed mean, $\overline{x}_{MC}$, for a generated lifetime of τ_{MC}:

$$\tau_\tau = \tau_{MC} \times \frac{\overline{x}_{meas}}{\overline{x}_{MC}} \; . \tag{4}$$

Monte Carlo checks on this technique, given in [5], included verification of the linearity and zero-intercept assumptions implicit in the above equation. The uncertainty from extrapolation was made negligible by use of a Monte Carlo generator lifetime which is very close to the measured value. Figure 1 shows the impact parameter distribution for those 1991 data which have silicon detector information included. The three components of 1990 data, 1991 data without silicon hits, and 1991 data with silicon-hit tracks were treated separately, and the individual lifetime measurements were combined. Table 2 shows the results for each component. The combined weighted average for the one-prong analysis, uncorrected for residual backgrounds, is 294.0 ± 7.0 fs, where only the statistical error is given. This statistical error contains a small contribution, of about 2.1 fs in quadrature, due to limited Monte Carlo statistics.

Several checks were made on the stability and internal consistency of the one-prong τ lifetime measurement. The τ selection cuts were checked to ensure that no significant bias to the measurement results from their application. The data were divided into groups according to azimuthal angle, $|\cos\theta_{\rm thrust}|$, event visible energy, and number of tracks in the opposite hemisphere. All results from the various subgroups are consistent. The azimuthal angle check,

[1] This correction becomes significant only at large values of the total trim. For a 10% trim factor, the corrected formula gives 2.4% statistical error on the trimmed mean, to be compared with the 2.3% predicted from the uncorrected formula.

done separately for each of the three data sets, is particularly important in that the effective impact parameter resolution changes significantly among the samples due to both the effect of the LEP beam shape and the change between gas and silicon vertex detectors. The analysis was repeated including electromagnetic calorimeter information in the thrust axis calculation, giving results consistent with those using only charged tracks for the thrust axis determination. The lifetimes obtained from data taken at center-of-mass energies above, below, and on peak are in agreement.

In that portion of the data with both vertex detectors present, the lifetimes obtained from the same events analysed with or without the silicon information are in good agreement. Because the width of the impact parameter distribution is dominated by the horizontal size of the beamspot, the improvement in the tracking resolution from the addition of the silicon hits results in only a modest gain in the statistical precision of the combined measurement, with 2.6% statistical error on the result without silicon, and 2.4% error if silicon information is included.

An impact parameter analysis using tracks from three-prong decays was performed as a check. The same quality cuts as described in the τ-pair event selection above were used to select tracks from three-prong decay candidates. Comparison of the trimmed mean for these distributions with the corresponding Monte Carlo predictions produces the result 297.3 ± 10.9 fs, where only the statistical error is given. This value is consistent both with the one-prong impact parameter measurement and the decay length measurement described in the following section. Because this determination of the lifetime from three-prong decays is less precise than the result from the decay length measurement, and also for simplicity of combination of the otherwise statistically-independent one-prong and three-prong lifetime determinations, this result is considered only as a check and is not used in the final measurement.

Several sources of systematic uncertainty have been evaluated. All resolution effects such as beamspot size uncertainty, vertex detector calibration and track resolution affect the width of the signed impact parameter distribution but do not appreciably shift the mean. However, although the trimmed mean is found to be rather stable under variations of the impact parameter resolution, slight differences between the shapes of the data and Monte Carlo impact parameter distributions can cause systematic shifts in the lifetime. The effect of a shape difference is a smooth change in the measured lifetime as the trim factor is varied. The variation of 1.1% in the measured lifetime when the trim factor was varied over the 1% to 30% range is taken as the systematic error arising from the combined effects of detector resolution, beam position and beam size uncertainties.

In addition several direct checks of beam and detector resolution effects have been carried out. A change of 25 μm in both the x and y beam centroid positions changed the lifetime by 0.1%. Increasing the horizontal beam width by 10 μm gave a 0.5% change. The component of the impact parameter resolution due to track reconstruction was varied by $\pm 10\%$ in the Monte Carlo, equivalent to roughly two times the uncertainty with which the data and Monte Carlo tracking resolution are matched, with less than 0.1% change in the lifetime. Each of these measurements corresponds to the variation of a different component of the overall impact parameter resolution. The error obtained above from varying the trim factor is taken to include these effects.

Effects of biases in the thrust axis direction due to possible detector miscalibrations were

measured by applying a Gaussian smearing to the thrust axis ϕ direction.[2] The width of this smearing, 0.5 mrad, corresponds to an amount several times the angular resolution in ϕ. The resulting shift in the measured lifetime, 0.1%, is assigned as a systematic error.

Uncertainty in the branching fractions of the various τ decay modes leads to a systematic uncertainty in the overall trimmed mean for the Monte Carlo. Each decay mode branching ratio was varied by twice its current world average uncertainty, to allow for extra shifts in their values to compensate the τ one-prong branching fraction anomaly [15]. The maximum effect arises from variation of $\mathrm{BR}(\tau \to \rho(\mathrm{K}^*)\nu_\tau)$, with a current world average of $24.4 \pm 0.6\%$. This leads to a systematic error contribution on the lifetime determination of 0.7%. Variations of the assumed mass and width of the a_1 resonance had no effect on the measured lifetime. The mean impact parameter is invariant under the small difference in τ masses between the value used in Monte Carlo generation and the recent measurements [3, 4].

As shown in Table 1, a background of $1.51 \pm 0.51\%$ combined Bhabha, μ-pair, two-photon, and multihadron tracks remains in the one-prong sample. Although these are expected to have zero average impact parameters, the trimmed mean cut points as determined by the predominant τ signal are asymmetric about zero, and so induce a non-zero trimmed mean from the background component. The mean values obtained by applying the same 10% trim window from the data distribution to Monte Carlo background samples were 15.1 ± 4.6 μm for the μ-pair component, and 25.8 ± 6.9 μm for the two-photon component. These contaminations have trimmed means less than that of the τ signal, leading to an upward correction for the measured lifetime based on the relative proportion of each source remaining in the final trimmed mean sample. This correction is $+0.82 \pm 0.28\%$, where the systematic error is estimated by varying the background fraction within the uncertainty given in Table 1.

In summary, the following systematic errors are assigned:

Variation of trim factor	
(includes detector resolution and beam size effects)	$\pm 1.1\,\%$
Monte Carlo decay mode branching ratios	$\pm 0.7\,\%$
Thrust axis direction biases	$\pm 0.1\,\%$
Background fractions	$\pm 0.3\,\%$
Total systematic error:	$\pm 1.3\,\%$

The final result for the one-prong measurement of the lifetime is then

$$\tau_1 \;=\; 296.4 \;\pm\; 7.1\ (\mathrm{stat}) \;\pm\; 3.8\ (\mathrm{sys})\ \mathrm{fs}\ . \tag{5}$$

[2] The impact parameter, measured in the x-y plane, is independent of track θ information.

6 Lifetime measurement by the decay length method

The decay length measurement is an attempt to determine the true τ flight distance from three-prong decays. Thrust hemispheres containing exactly three tracks of total charge ± 1 were selected, and the tracks were fitted to a common vertex in the x-y plane. A total of 4028 such vertices were reconstructed from the full 1990 and 1991 data samples. As for the one-prong measurement, estimates of the production point and the τ flight direction were taken from the average beam position and the charged track thrust axis, while the reconstructed vertex of the three charged tracks measured the actual τ decay position. These components were then combined in a best fit for the x-y projection of the decay length. The three-dimensional decay length and its error were formed by using the thrust axis polar angle. The decay lengths were normalized to a reference center-of-mass energy $\sqrt{s} = 91.160$ GeV, including initial state radiation correction factors, determined from the Monte Carlo, for each center-of-mass energy used during scans about the Z^0 peak. A maximum likelihood fit was applied to give the most probable decay length and its uncertainty, which was then converted into a lifetime measurement.

The measurement of the reconstructed vertex position can be quite susceptible to systematic errors arising from detector miscalibrations. Since the original OPAL τ lifetime publication [5], an improved correction has been developed for adjusting the positions of hits which follow the initial hit recorded on a particular vertex drift chamber anode wire. The new correction for secondary hits accounts for the ionization caused by all tracks passing through the detector between a previous hit and the anode plane, including those tracks which follow too closely in time behind a preceding track to register hits in the vertex chamber. In addition, the sensitivity of the decay length analysis to details of multi-hit corrections has been significantly reduced, by requiring at least two of the three tracks of the vertex to be "well-measured". Here, well-measured tracks are either those which include more first hits in the vertex drift chamber than secondary hits, or which contain at least one silicon microvertex detector hit. The vertices selected by this criterion are in fact those which give the smallest decay length uncertainties. The addition of this quality cut entails a large loss of efficiency in the data taken before installation of the silicon detector, in which case only 40% of the vertices are selected. However, for the data with silicon present, the cut is nearly 90% efficient. This increase in efficiency is more important for improving the statistical precision of the decay length measurement than the enhanced resolution provided by the silicon detector: for samples of exactly the same number of events the addition of silicon hits in the tracking reduces the statistical error from the fit by just 8%, to a value approaching the theoretical minimum, $l_0/\sqrt{N}$, attainable with unlimited precision.

After imposing the requirement that at least two of the three tracks of the vertex be well-measured, 2609 vertices (65%) remained. A cut of 1% on the vertex fit probability rejected a further 497 (15%) of these vertices with suspected reconstruction errors. The narrow opening angles of τ decays at Z^0 energies, which average 90 mrad, lead to error ellipses from the vertex fits having high aspect ratios. The error matrix components of the selected vertices along/perpendicular to the thrust axis averaged 1600/60 μm in the data without silicon tracking, and 1150/30 μm in the data with silicon vertex detector information available.

In order to reduce the uncertainty on the measured τ decay length and to discriminate

against poorly-reconstructed decays, the two-dimensional decay vertex and error ellipse were combined with the beam spot position and size and with the thrust axis direction constraint in a least-squares fit to determine the most probable τ flight length and its error [5]. A probability cut of 1% was imposed for the fit, resulting in a 5% reduction of the sample size to a total of 2212 decay length measurements. The two-dimensional decay length errors from this fit are about 7% less than the major axis of the vertex error ellipse stated above. However, the projection to three dimensions increases the decay length errors to an average of 1900 μm in the data with drift chamber tracking only, and 1300 μm in the data which have silicon vertex chamber information.

The distribution of decay lengths was taken to be the convolution of an exponential with Gaussian resolution functions of widths equal to the decay length errors. The probability of observing a single decay of length l_i and uncertainty σ_i is

$$\begin{aligned} P(l_i,\sigma_i;l_0,s_0) &= \frac{1}{l_0 s_0 \sigma_i \sqrt{2\pi}} \int_0^\infty e^{-x/l_0} e^{-\frac{(x-l_i)^2}{2 s_0^2 \sigma_i^2}} \, dx \\ &= \frac{1}{2l_0} \, \exp\!\left[\frac{s_0^2\sigma_i^2}{2l_0^2} - \frac{l_i}{l_0}\right] \, \mathrm{erfc}\!\left[\frac{1}{\sqrt{2}}\left(\frac{s_0\sigma_i}{l_0} - \frac{l_i}{s_0\sigma_i}\right)\right] , \end{aligned} \tag{6}$$

where in addition to the parent decay length l_0, a scale factor s_0 for the decay length errors, σ_i, was included as a fit variable. This scale factor provides an allowance for the possibility that the decay length errors were incorrectly estimated. The maximum likelihood fit minimizes the negative sum of the log of the probabilities for all decay lengths and errors. Because this method is sensitive to decay lengths in the far tails of the distribution a window cut of -1.0 cm $< l_i < +2.0$ cm was applied, which eliminated 0.5% of the decay length candidates. A renormalization factor for the probability function accounts for the reduced range of the decay length in the above integral [17, 18]. Finally, a cut of $\sigma_i < 0.6$ cm was applied to the decay length errors, which eliminated 1.1% of decays which have relatively poor resolving power for the maximum likelihood fit.

A total of 2048 decay length measurements survived all the cuts. The contributions from 1990 data, and 1991 data, with and without the silicon detector available, are given in Table 3. Approximately 68% of the full sample came from the data with the silicon vertex detector. The decay lengths and error scaling factors for the separate fits are also given in Table 3. The overall weighted average decay length is

$$l_0 \;=\; 0.2161 \;\pm\; 0.0057 \text{ cm} \, . \tag{7}$$

The overall result can also be obtained from a single maximum likelihood fit to the combined set of 2048 vertices, which is shown in the distribution of Figure 2. The average decay length resulting from this fit, 0.2162 $\pm$ 0.0057 cm, agrees quite well with the result obtained by a weighted average of the fitted decay lengths from the three component data sets. The result of the single fit is illustrated by the overlaid curve of Figure 2. The fitted average decay length is converted to a measured lifetime by scaling according to the reference energy and the τ mass. From the relationship $l_0 = \beta\gamma c\tau_\tau$, using the weighted average of the two recent high-precision mass determinations [3, 4], $m_\tau = 1776.9 \pm 0.5$ MeV/c^2, there results

$$\tau_\tau \;=\; (1301.4 \text{ fs/cm}) \;\times\; l_0 \, . \tag{8}$$

At this point, before the corrections described below, the lifetime from the three-prong vertices is 281.2 ± 7.4 fs.

Checks were performed, dividing the data into subsets according to the τ direction azimuthal and polar angle, vertex and decay length fit probabilities, three-prong charge, and number of tracks in the opposite hemisphere. The decay lengths from all subsets are consistent. The maximum likelihood window cut was varied within the range $[-3.0, +3.0]$ cm, with consistent results for all choices of window. For tracks with silicon hits, test fits were done in which the r-ϕ covariance matrix elements of the tracks extrapolated from the drift chambers into the silicon detector were increased by factors up to 1.6, the maximum estimated scaling factor for these elements, to check for the effects of improper weighting of tracks in the outer detectors relative to the silicon hits. No trends were observed. Measurements using electromagnetic calorimeter information in the thrust axis determination, or with an event axis determined by the summed momentum vector of the three charged tracks produce statistically consistent results.

In order to address the possibility of pattern recognition mistakes in dense track environments leading to a bias towards longer measured lifetimes [19], the decay length was measured as a function of both the minimum and maximum separations between tracks of the three-prong decay vertex. No systematic trend to higher decay lengths with smaller opening angles is evident in either the divisions by minimum track separation or in the divisions by maximum opening angle.

Systematic error contributions from several sources have been estimated. Residual calibration uncertainties from the multi-hit corrections are greatly reduced by the "two good track" requirement. We estimate an uncertainty of 0.2% from this source. Uncertainties in vertex drift chamber calibration constants are due to the effect of a 0.08% uncertainty in the drift velocity, which leads to a 0.5% systematic error in the decay length. The effects of tracks passing through the highly nonlinear drift velocity region near the anodes are taken into account by including as a systematic error the 0.8% shift in the result which is observed when vertices containing such tracks are excluded. The quadrature sum of these effects is 1.0%.

Silicon microvertex detector alignment uncertainties were studied in the course of determining its calibration constants. Residual uncertainties are estimated by introducing incoherent shifts of 100 μm in the nominal radial positions of each ladder, and by coherent shifts of 50 μm. These effects contribute 0.7% and 0.4% uncertainty, respectively, in the data with silicon detector information. The effect of varying the silicon intrinsic resolution from 10 μm to 20 μm is a 0.4% change in the measured decay length. After scaling for the two-thirds proportion of data with silicon information present, the quadrature sum of all three effects is 0.6%.

The effect of the photon conversion finding efficiency was checked by use of alternative conversion finding schemes having efficiencies of up to 75% higher than the algorithm used in this analysis. No systematic shift in the lifetime as a function of the conversion finding efficiency is observed. The results of all conversion rejection schemes, including no rejection at all, are consistent within their 1.2% statistical uncertainties, and the maximum observed variation of 0.6% is taken as a systematic error.

Effects of systematic shifts in the thrust axis determination have been investigated by including systematic shifts in the θ and ϕ track parameters used in the decay length determination. The inclusion of up to eight times the tracking ϕ uncertainty produces no change in the result.

The shift observed as a result of coherently shifting the track θ-values by an amount equivalent to their typical precision of determination leads to a maximum bias estimate from this source of 0.4%.

Variations in the beam spot position and size have been examined for their effect on the measurement. An allowance is made for shifts of up to 25 μm in both the x- and y-centroid positions. This leads to a 0.5% uncertainty in the fitted decay length. Variations of up to 10 μm in the horizontal beam width were investigated, giving rise to a 0.3% change in the result. The combination of the two effects contributes 0.6% to the systematic uncertainty.

The background contamination was checked directly by processing Monte Carlo multihadron events through the same analysis chain as the data. The estimated background remaining in the maximum likelihood fit sample is $0.4 \pm 0.4\%$. This component is taken to have zero average decay length, giving rise to a correction of $+0.4\%$ for the lifetime, together with a systematic uncertainty of the same amount. This uncertainty is due almost entirely to the uncertainty with which such low-multiplicity events are modelled in the Monte Carlo.

The corrections for the measured decay length due to initial state radiation were determined with Monte Carlo data samples to an uncertainty of $\pm 0.1\%$, which is taken as a systematic error contribution.

A small bias is created upon introduction of the 1% probability cut for the decay length fit, which is a result of the use of a rigid thrust axis constraint when combining the fitted vertex and error ellipse with the beam position and envelope. The undetected neutrino naturally causes some small deviation of the thrust axis from the true τ flight direction, of average 15 mrad. Because of this, longer-lived τ vertices become more susceptible to failing the probability cut. This effect is especially pronounced in horizontally-lying decays, where the dimensions of both the beam and vertex error ellipses perpendicular to the thrust axis direction are very small. The magnitude of the effect is evaluated in the Monte Carlo, leading to a correction factor of $+1.4 \pm 1.0\%$. The 1.0% uncertainty encompasses the uncertainty on the bias from this effect and from other potential sources of bias which are simulated by the Monte Carlo.

The systematic errors are summarized as follows:

Vertex drift chamber calibration	$\pm 1.0\,\%$
Silicon detector alignment	$\pm 0.6\,\%$
Conversion finding efficiency	$\pm 0.6\,\%$
Thrust axis direction biases	$\pm 0.4\,\%$
Beam position and size variations	$\pm 0.6\,\%$
Multihadron background fractions	$\pm 0.4\,\%$
Radiative corrections	$\pm 0.1\,\%$
Measurement biases	$\pm 1.0\,\%$
Total systematic error:	$\pm 1.8\,\%$

The final result for the three-prong measurement of the lifetime is then

$$\tau_3 \;=\; 286.3 \;\pm\; 7.4\ (\text{stat}) \;\pm\; 5.2\ (\text{sys})\ \text{fs}\ . \tag{9}$$

A separate analysis was performed using only those three-prong decays in which at least one microvertex detector hit is associated with each track. This analysis serves as an independent check of the three-prong measurement, and as an additional check on possible systematic effects arising in the outer tracking chambers.

The event selection and analysis procedure were similar to those described above, resulting in 1291 three-prong decays in which all tracks have at least one silicon hit. The τ-decay vertex was found by a χ^2 minimization involving the three tracks as determined by the central jet and vertex chambers, together with the distance of all silicon hits to these tracks, subject to the constraint that the tracks originated from a common decay vertex. This method was chosen because it allowed the effects of the silicon microvertex detector and of the gas tracking chambers to be studied separately. Multiple scattering effects were included in the fit.

The reconstructed vertices were combined with the τ direction as determined by the summed momentum of the three charged tracks of the decay, and the beam position and envelope in a best fit for the decay length and its error. The decay lengths and errors were converted to three-dimensional quantities using the three-prong summed-momentum polar angle. The same radiative corrections and center-of-mass energy corrections as described above were applied, and the resulting decay lengths were subjected to a maximum likelihood fit. No decay length window cuts were applied for this fit. A total of 867 vertices passed the probability and decay length error cuts, with a result

$$l_0 \;=\; 0.2201 \;\pm\; 0.0080 \text{ cm}, \quad s_0 \;=\; 1.01 \;\pm\; 0.05 \;. \tag{10}$$

Systematic error effects similar to those outlined above were evaluated. After transforming the decay length by the overall scale factor given above, the lifetime measured by the second three-prong analysis is

$$\tau_3^{SI} \;=\; 288.5 \;\pm\; 12.0 \text{ (stat)} \;\pm\; 6.7 \text{ (sys) fs}. \tag{11}$$

The larger systematic error relative to that given above is due to a greater sensitivity to silicon alignment effects, associated with the requirement that all three tracks have silicon hits.

This result is in agreement with the previous three-prong decay length lifetime measurement. However, it is not used in the final lifetime determination because of the large overlap of the sample with that analysis and its larger statistical error.

7 Lifetime measurement in 1-3 τ-pair decays

An independent check to both the one-prong and three-prong analyses was performed using a novel technique which is independent of beam position information. This technique has been applied only to the subset of data with silicon tracking available.

Within the 1-3 τ-pair decay topology, we first define variables as illustrated in Figure 3a. Working only in the x-y plane, the displacement vector $\vec{d}_{13}$ is taken from the three-prong decay vertex to the point of closest approach of the one-prong decay track. Assuming the two

τ particles are back-to-back, the magnitude of $\vec{d}_{13}$ relates to the sum of the τ decay lengths, l_1 and l_3 as

$$|\vec{d}_{13}| \;=\; (l_1 + l_3)\sin\theta|\sin\Delta\phi_1|, \tag{12}$$

where θ is the polar angle of the event and $\Delta\phi_1$ is the opening angle of the one-prong decay momentum vector with respect to the true τ flight direction.

Because the angular opening $\Delta\phi_1$ is not directly observable, the acoplanarity angle, $\Delta\phi$, defined as the azimuthal difference between the one-prong and summed three-prong momentum vectors, $\vec{p}_1$ and $\vec{p}_3$, is introduced. The facts that $\Delta\phi_1$ is small, and that the rms deviation of $\Delta\phi$ is dominated by that of $\Delta\phi_1$ rather than that of $\Delta\phi_3$ (the angular opening of $\vec{p}_3$ with respect to its parent τ flight direction), lead to the relations: $\sin\Delta\phi_1 \approx \Delta\phi_1 \approx \Delta\phi$. For a given value of $\sin\theta\ \Delta\phi$, with $(l_1 + l_3)$ replaced by twice the average decay length, one obtains for an ensemble of 1-3 τ-pair decays:

$$\langle\delta_{13}\rangle \approx 2\beta\gamma c\tau_\tau \sin\theta\ \Delta\phi\ , \tag{13}$$

where δ_{13} is a signed impact parameter, having the same magnitude $|\vec{d}_{13}|$ but using the sign of the z-projection of $\vec{d}_{13}\times\vec{p}_1$, and the sign of $\Delta\phi$ is correspondingly taken from the z-projection of $\vec{p}_1\times\vec{p}_3$. This equation can be considered as a linear function of the average impact parameter with respect to a new variable $X \equiv 2\beta\gamma c\sin\theta\Delta\phi$, with the τ lifetime entering directly as the slope. A similar technique has been introduced for extracting the lifetime from 1-1 τ decays [20]. In that case, the difference of one-prong impact parameters is used to eliminate the dependence on the poorly estimated τ flight direction in 1-1 τ decays. The beam spot uncertainty, however, contributes doubly to the measured quantity in the analysis and degrades the statistical precision as a result.

Tau-pair events were selected as described above. After removal of photon conversions, candidate 1-3 τ-pair decays were required to have silicon hits on the one-prong decay track, and at least two of the three-prong decay tracks. The χ^2 probability of the fitted three-prong decay vertex was required to be greater than 1%. After these cuts, 1224 1-3 τ-pair decay candidates remained.

The decay signed impact parameters, δ_{13}, were then binned in X, and for each bin the 10% trimmed mean and error were calculated as described above in the impact parameter measurement. The resulting distribution is shown in Figure 3b, together with a fit to the linear form $Y = AX + B$. Since the fitted $B = -0.4 \pm 2.9$ μm is consistent with zero, the fit was redone with variable slope only giving $A = 241.7 \pm 9.3$ fs. This result must then be corrected for the assumption $\sin\Delta\phi_1 \approx \Delta\phi$, as well as for the effect of trimming. A calibration curve was constructed from Monte Carlo τ data generated with various input τ lifetimes. Comparison of the lifetimes obtained by the method with the input generator values gives the linear calibration factor, $a \equiv \tau_\tau(\mathrm{fit})/\tau_\tau(\mathrm{input}) = 0.8282 \pm 0.0090$. Applying this calibration factor to A yields the result $\tau_\tau = 291.9 \pm 11.2$ fs.

This method has been evaluated for potential biases in the measured lifetime. Three effects cause significant shifts which are applied to find the final measurement: the residual multihadronic background results in a shift of $+0.2 \pm 0.1$ %; impact parameter resolution modelling, $+0.3 \pm 0.2$ %; and the energy dependence of radiative corrections, $+0.1 \pm 0.1$ %.

Systematic errors include those arising from uncertainties in the Monte Carlo used to extract the calibration factor, and detector effects similar to those evaluated for the three-prong decay

length analysis. These are summarized as:

Three-prong decay modelling uncertainties	$\pm 0.5\,\%$
One-prong branching ratios	$\pm 0.1\,\%$
Thrust axis direction biases	$\pm 0.4\,\%$
Tau polarization and radiation	$\pm 0.3\,\%$
Photon conversion, K^0 rejection	$\pm 0.1\,\%$
Silicon detector alignment	$\pm 1.5\,\%$
Impact parameter resolution	$\pm 0.2\,\%$
Multihadron background fractions	$\pm 0.1\,\%$
Monte Carlo statistics	$\pm 1.1\,\%$
Total systematic error:	$\pm 2.0\,\%$

The final result for the lifetime using the 1-3 τ-pair decays is then

$$\tau_{13} \;=\; 293.4 \;\pm\; 11.2\ (\text{stat}) \;\pm\; 5.8\ (\text{sys})\ \text{fs}\ . \tag{14}$$

This result is consistent with both the one-prong and three-prong measurements. Because of its overlap with the data used for both those measurements, it is presented here as a check on those results and is not considered in determining the final value for the lifetime. In future measurements, this technique may become more useful if limitations on the precision due to the beam size or location estimation become greater than those arising from the limitations of detector resolution.

8 Summary

After combining the statistical and systematic uncertainties for each of the one-prong and three-prong analyses in quadrature, the weighted average lifetime from (5) and (9) is:

$$\tau_\tau \;=\; 291.9 \;\pm\; 5.1\ (\text{stat}) \;\pm\; 3.1\ (\text{sys})\ \text{fs}. \tag{15}$$

We have treated the systematic error contributions for the two analyses as uncorrelated. The background contamination uncertainty is a small effect which is orthogonal between the two analyses, as seen from Table 1. The thrust axis resolution component of the systematic errors gives likewise a small contribution to the error in each analysis, and is nearly decoupled between the analyses in that 1-3 τ-pair decays contribute only 14% of the tracks used in the one-prong measurement.

We find a result which is slightly lower than the current world average 305 ± 6 fs [21]. There is good agreement with other recent τ lifetime determinations [22, 23]. Our value in fact points to a resolution of the discrepancy between the τ lifetime, mass, and leptonic branching ratios. When combined with OPAL measurements of the τ leptonic branching fractions [24], the recent τ mass determinations [3, 4], and the assumption of lepton universality, equation (1) predicts a lifetime $\tau_\tau = 283.0 \pm 7.5$ fs, in agreement with our result. Equation (1) can also be rewritten as a test of lepton universality. In this case we find

$$\frac{g_\tau}{g_\mu} = 0.985 \pm 0.017, \tag{16}$$

consistent with the lepton universality hypothesis.

9 Acknowledgements

It is a pleasure to thank the SL Division for the efficient operation of the LEP accelerator, the precise information on the absolute energy, and their continuing close cooperation with our experimental group. In addition to the support staff at our own institutions we are pleased to acknowledge the
Department of Energy, USA,
National Science Foundation, USA,
Texas National Research Laboratory Commission, USA,
Science and Engineering Research Council, UK,
Natural Sciences and Engineering Research Council, Canada,
Fussefeld Foundation,
Israeli Ministry of Energy,
Israeli Ministry of Science,
Minerva Gesellschaft,
Japanese Ministry of Education, Science and Culture (the Monbusho) and a grant under the Monbusho International Science Research Program,
German Israeli Bi-national Science Foundation (GIF),
Direction des Sciences de la Matière du Commissariat à l'Energie Atomique, France,
Bundesministerium für Forschung und Technologie, FRG,
National Research Council of Canada, Canada,
A.P. Sloan Foundation and Junta Nacional de Investigação Científica e Tecnológica, Portugal.

References

[1] B.C. Barish and R. Stroynowski, Phys.Rep. **157** (1988) 1.

[2] W.J. Marciano, Phys.Rev. **D45** (1992) R721.

[3] BES Collaboration, J.Z. Bai et al., Phys.Rev.Lett. **69** (1992) 3021.

[4] ARGUS Collaboration, H. Albrecht et al., Phys.Lett. **B292** (1992) 221.

[5] OPAL Collaboration, P.D. Acton et al., Phys.Lett. **B273** (1991) 355.

[6] OPAL Collaboration, K.Ahmet et al., Nucl. Instrum. and Meth. **A305** (1991) 275.

[7] P.P. Allport et al., *The OPAL Silicon Microvertex Detector*, to be published in Nucl. Instrum. and Meth.

[8] OPAL Collaboration, G. Alexander et al., Z.Phys. **C52** (1991) 175.

[9] T. Sjöstrand, Comp.Phys.Comm. **39** (1986) 347; JETSET, Version 7.2.

[10] M. Bohm, A. Denner and W. Hollik, Nucl. Phys. **B304** (1988), 687;
F. A. Berends, R. Kleiss, W. Hollik, Nucl. Phys. **B304** (1988), 712.

[11] R. Bhattacharya, J. Smith, G. Grammer, Phys. Rev. **D15** (1977) 3267;
J. Smith, J.A.M. Vermaseren, G. Grammer, Phys. Rev. **D15** (1977) 3280.

[12] S. Jadach et al., Comp.Phys.Comm. **66** (1991) 276; KORALZ, Version 3.8.

[13] J. Allison et al., Nucl. Instrum. and Meth. **A317** (1992) 47.

[14] The a_1 mass was set to 1251 MeV/c^2, and its width to 599 MeV, to produce agreement with the data of:
H. Kolanoski, ARGUS Collaboration, DESY-91-145C (1991).

[15] Particle Data Group, J. J. Hernández et al., Phys.Lett. **239** (1990) 1.

[16] H. N. Nelson, *Design and Construction of a Vertex Chamber and Measurement of the Average B Hadron Lifetime,* (Ph.D. thesis), SLAC-Report-32 (1987).

[17] A. G. Frodesen, O. Skjeggestad, and H. Tofte, *Probability and Statistics in Particle Physics*, Universitetsforlaget, Bergen, Norway (1979).

[18] C. Kleinwort, *Bestimmung der Lebensdauer des τ-Leptons mit dem JADE-Detektor,* (Ph.D. thesis), Universität Hamburg (1988).

[19] C. K. Jung, *Experimental explanation of tau lepton decay puzzle: Discrepancy between the measured and theoretical τ lifetimes*, SBHEP-92-1, May 1992, submitted to Phys.Rev.

[20] ALEPH Collaboration, D. Decamp et al., Phys.Lett. **B279** (1992) 411.

[21] Particle Data Group, K. Hikasa et al., Phys.Rev. **D45** (1992) S1.

[22] ALEPH Collaboration, D. Buskulic et al., *A Precise Measurement of the τ Lepton Lifetime*, CERN-PPE/92-186 (1992), submitted to Phys.Lett.B.

[23] CLEO Collaboration, M. Battle et al., Phys.Lett. **B291** (1992) 488.

[24] OPAL Collaboration, G. Alexander et al., Phys.Lett. **B266** (1991) 201.

Tables

		one-prong	three-prong
data	number	25579	4028
back-grounds	multihadrons (%)	0.06 ± 0.30	0.40 ± 0.40
	e^+e^- (%)	0.14 ± 0.28	0
	$\mu^+\mu^-$ (%)	0.81 ± 0.22	0
	two-photon (%)	0.50 ± 0.20	0
	total (%)	1.51 ± 0.51	0.40 ± 0.40

Table 1: Numbers of one-prong and three-prong candidates and the percentages of backgrounds, with their combined statistical and systematic uncertainties.

component	number of tracks	trimmed mean (μm)	MC trimmed mean (μm)	measured lifetime (fs)
1990 data	7537	45.2 ± 1.9	47.2 ± 0.7	290.7 ± 13.2
1991 without silicon	7148	47.4 ± 2.2	47.6 ± 0.5	302.3 ± 14.5
1991 with silicon hits	10894	44.7 ± 1.5	46.5 ± 0.5	291.9 ± 10.1
combined	25579	–	–	294.0 ± 7.0

Table 2: Lifetime measurements from the trimmed means of the three component samples for the one-prong analysis. Only the statistical errors are given.

component	no. vertices reconstructed	no. vertices in fit	decay length (cm)	error scale factor
1990 data	1138	387	0.237 ± 0.016	1.081 ± 0.070
1991 pre-silicon	791	264	0.209 ± 0.017	1.262 ± 0.084
1991 with silicon	2099	1397	0.2135 ± 0.0065	0.990 ± 0.038
combined	4028	2048	0.2161 ± 0.0057	–

Table 3: Lifetime measurements from the decay lengths of the three component samples and the combined sample for the three-prong analysis. Only the statistical errors are given.

Figure Captions

Figure 1: Impact parameter distribution for the 1991 data with silicon information present, in linear and log scales. Arrows indicate the cut points for the 10% trimmed mean. The histogram shows the Monte Carlo prediction for a lifetime of 303 fs.

Figure 2: Decay length distribution for the combined 1990 plus 1991 data set, where information from the silicon microvertex detector is included when available. The overlaid curve indicates the result of a global maximum likelihood fit for the average τ decay length.

Figure 3: Illustration of the parameter definitions for the 1-3 τ decay lifetime measurement, upper diagram. The lower plot gives the 10% trimmed mean of the signed impact parameter, as a function of the variable X, defined in the text, together with the result of a linear fit.

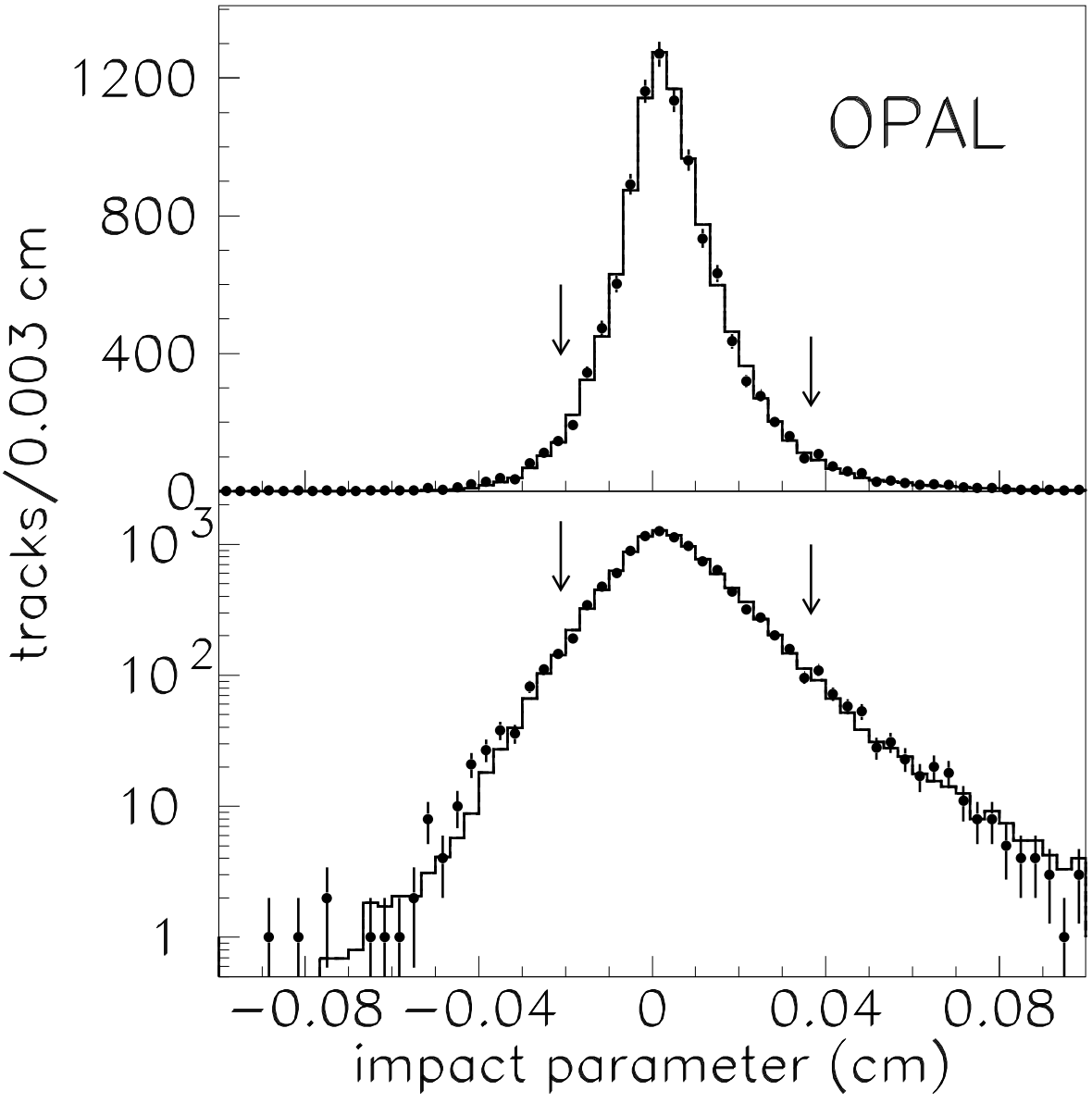
OPAL
1200
800
400
0
10^3
10^2
10
1
tracks/0.003 cm
−0.08
−0.04
0
0.04
0.08
impact parameter (cm)

Figure 1:

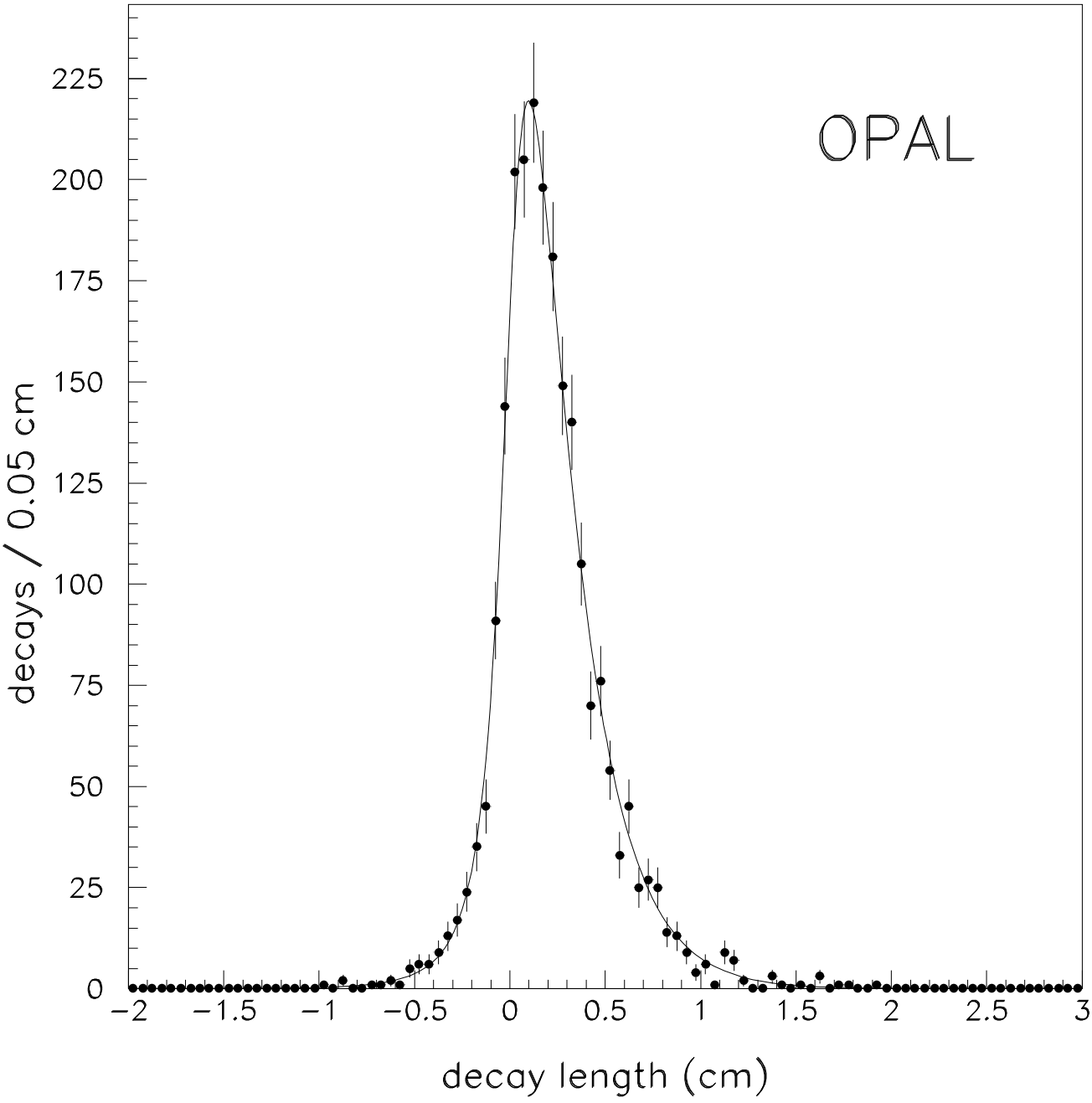
OPAL
decays / 0.05 cm
decay length (cm)
0
25
50
75
100
125
150
175
200
225
−2
−1.5
−1
−0.5
0
0.5
1
1.5
2
2.5
3

Figure 2:

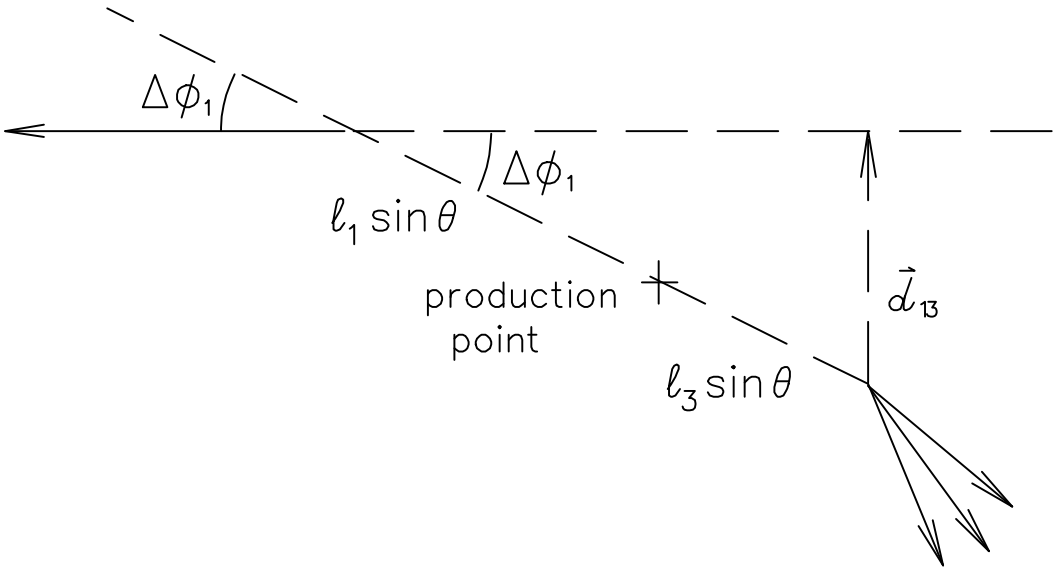
$\Delta\phi_1$
$\Delta\phi_1$
$\ell_1 \sin\theta$
production
point
$\vec{d}_{13}$
$\ell_3 \sin\theta$

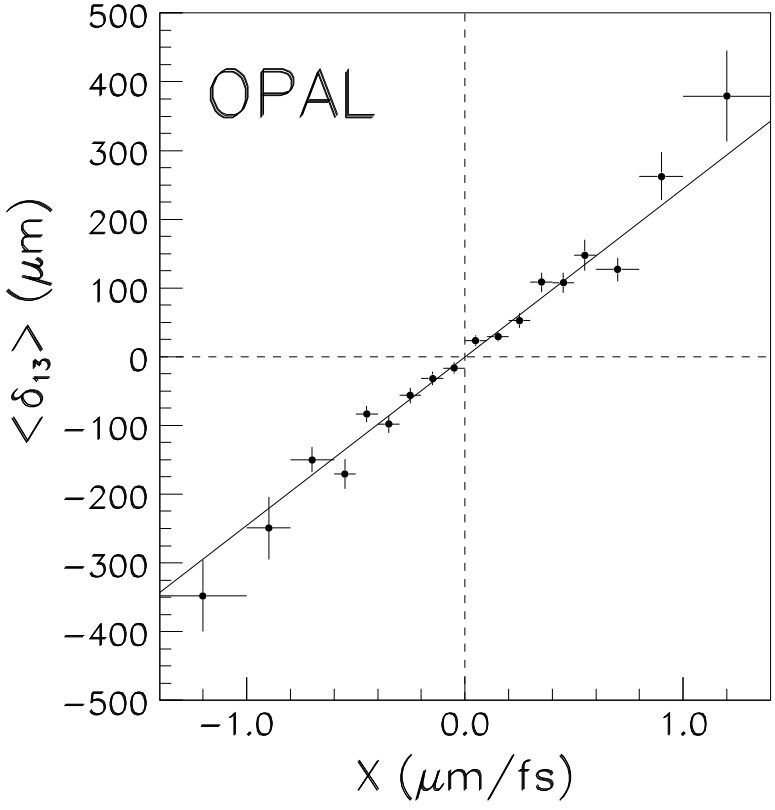
OPAL
$\langle \delta_{13} \rangle$ (μm)
X (μm/fs)
500
400
300
200
100
0
−100
−200
−300
−400
−500
−1.0
0.0
1.0

Figure 3: